Journal of Endourology

DOI: 10.1089/end.2019.0564

DISCREPANCY BETWEEN STONE AND TISSUE MINERAL TYPE IN PATIENTS WITH IDIOPATHIC URIC ACID STONES

Andrew P. Evan[a], Fredric L. Coe[b], Elaine M. Worcester[b], James C. Williams, Jr.[a], Joshua Heiman[a], Sharon Bledsoe[a], Andre Sommer[c], Carrie L. Philips[d], and James E. Lingeman[e]

a. Department of Anatomy and Cell Biology, Indiana University School of Medicine, Indianapolis, IN

b. Department of Medicine, University of Chicago, Chicago, Illinois

c. Department of Chemistry and Biochemistry, Miami University, Oxford, Ohio

d. Department of Pathology, Indiana University Health Partners, Indianapolis, IN

e. Department of Urology, International Kidney Stone Institute, Indiana University Health Partners, Indianapolis, IN

Evan (aevan@iupui.edu);

Coe (fredcoe@gmail.com);

Worcester (eworcest@uchicago.edu);

Williams (jwillia3@iupui.edu);

Heiman (joshmheiman@gmail.com);

Bledsoe (sbledsoe@iupui.edu);

Sommer (sommeraj@miamioh.edu);

Philips (cphilli3@iupui.edu);

Lingeman (jlingeman@iuhealth.org)

Running title: Papillary biopsy of idiopathic UA stone formers

---

This is the author's manuscript of the article published in final edited form as:

Evan, A. P., Coe, F. L., Worcester, E. M., Williams, J. C., Heiman, J., Bledsoe, S., ... & Lingeman, J. E. (2020). Discrepancy Between Stone and Tissue Mineral Type in Patients with Idiopathic Uric Acid Stones. Journal of Endourology. https://doi.org/10.1089/end.2019.0564

Corresponding Author:

Elaine Worcester, MD

University of Chicago Medicine

5841 South Maryland Avenue

Nephrology Section / MC 5100

Chicago, IL 60637

Phone: 773-702-7459

Fax: 773-702-5818

ABSTRACT

Objectives. To describe the papillary pathology found in uric acid (UA) stone formers, and to investigate the mineral form of tissue deposits.

Materials and Methods. We studied 8 UA stone formers treated with percutaneous nephrolithotomy. Papillae were imaged intra-operatively using digital endoscopy and cortical and papillary biopsies were taken. Biopsies were analyzed by light microscopy, micro-CT, and micro-infrared spectroscopy.

Results. As expected, urine pH was generally low. UA supersaturation exceeded 1 in all but one case, compatible with the stone material. By intraoperative imaging, the renal papillae displayed a heterogeneous mixture of plaque and plugging, ranging from normal to severe. All patients had mineral in ducts of Bellini and inner medullary collecting ducts, which was mainly apatite with lesser amounts of urate and/or calcium oxalate in some specimens. Papillary and cortical interstitial tissue injury was modest despite the tubule plugging. No instance was found of a stone growing attached to either plaque or plugs.

Conclusions. UA stone formers resemble those with ileostomy in having rather low urine pH while forming tubule plugs that contain crystals that can only form at pH values above those of their bulk urine. This discrepancy between tissue mineral deposits and stone type suggests that local tubular pH exceeds that of the bulk urine, perhaps because of localized tubule injury. The manner in which UA stones form, and the discordance between tubule crystals and stone type, remain open research questions.

Key Words: nephrolithiasis, uric acid, Randall's plaque, papilla

INTRODUCTION

We have described the renal papillary appearance and histopathology of idiopathic calcium oxalate (CaOx) stone formers (ICSF)[1] whose renal papillae contain interstitial deposits of apatite (Randall's plaque), appearing as white patches on papillae. CaOx stones may form as overgrowths on plaque. In contrast, idiopathic calcium phosphate (CaP) stone formers commonly plug inner medullary collecting ducts (IMCD) with deposits of apatite crystals, and produce modest amounts of plaque[2]. Stones may form as overgrowths on ductal deposits[3]. Most other types of stone formers display various mixtures of ductal plugging and plaque[4;5].

Patient with ileostomy may form uric acid (UA) stones, and both plaque and plugs (composed of apatite and monosodium urate) are found[6]. The mechanism of plugging is unclear given that ileostomy patients with highly acidic urine produce plugs of apatite and urates that are not stable at the urine pH.

We present here 8 patients who made idiopathic UA stones, including their surgical anatomy, papillary biopsy histopathology, micro-infrared spectroscopy of papillary deposits, and micro CT analysis of tissue deposits, and show that their papillary mineral deposits resemble those of ileostomy patients who make UA stones.

MATERIALS AND METHODS

Subjects

We report all eight patients from our series of over 300 biopsied patients with intraoperative imaging who formed stones containing greater than 40% UA and lacked any bowel disease to account for it (**Table 1**).

Clinical Laboratory Studies

All subjects collected two 24-hour urine samples post-operatively while eating a free choice diet and off medications that could affect stone formation. Stone risk analytes were measured and urine supersaturation (SS) calculated using methods detailed

elsewhere[7]. The mean of the two samples is reported in **Table 2**. Routine blood measurements were made for clinical purposes.

Tissue Analysis

Papillary mapping and biopsy protocol. During percutaneous nephrolithotomy all accessible papillae were mapped and graded after stone removal by the surgeon for four papillary characteristics (tubular deposits, pitting, papillary contour, and Randall's plaque), each on a 0-2 scale as previously described[8]. The scores for each characteristic were averaged for all papillae graded (**Table 3)**. Biopsies were taken from the upper pole, inter-polar, and lower pole papillae, and from cortex when possible[1]. Papillae were digitally imaged intra-operatively, and total surface area of each papilla was measured using the images. One of us outlined areas of white (Randall's) and yellow (visible tubule deposits) plaque as well as the entire papilla on one set of prints to obtain the percentage of coverage with each type of plaque[9]. The study was approved by the Institutional Review Board Committee for Indiana University Health Partners (#98-073).

Light microscopy. All specimens were immersed in 100% alcohol and fixed for a minimum of one week. After fixation and prior to tissue embedment, whole biopsies were analyzed by micro-CT. All biopsies were embedded in a 50/50 mixture of Paraplast Xtra (Fisher) and Peel-away Micro-Cut (Polysciences). A total of 21 papillary biopsies and 8 cortical biopsies were examined.

Papillary histopathology. Twelve serial sections were cut at 4µ and stained with the Yasue metal substitution method for calcium histochemistry[10], hematoxalin & eosin for routine histological examination, or the Masson Trichrome stain to determine sites of interstitial fibrosis at the light microscopic level. Sections were examined for the presence or absence of tubule plugs, interstitial Randall's plaque, and interstitial fibrosis (**Table 4**)

Cortical histopathology. A renal pathologist blinded to patient information performed a semi-quantitative analysis[7] using Jones' silver stained cortical sections. Tubular atrophy and interstitial fibrosis were independently scored on a scale of 0 to 3 (0 = none, 1 = mild or < 34% of sample, 2 = moderate or 34-66%, and 3 = severe or >66%). Glomerulosclerosis was defined as increased mesangial matrix with or without wrinkling,

thickening and/or collapse of glomerular basement membranes. The total number of glomeruli observed and the number of glomeruli with any degree of sclerosis were recorded (**Table 4**).

Micro-CT. All papillary biopsies underwent µCT analysis with the SkyScan 1172 (Kontich, Belgium) high-resolution desktop µCT system allowing non-destructive mapping of the location and size of the crystalline deposits within a biopsy specimen, as in our prior publication[11]. Sizes of mineral regions were measured in shadow images as previously described[4]. Mineral types were judged from relative values of X-ray attenuation[12]

Micro-FTIR. Biopsies were cut (~5 µm thick) and mounted on low-E glass slides (Kevley Technologies, Chesterland, Ohio) for attenuated total internal reflection (ATR) imaging analysis. A serial section stained with Yasue silver replacement was employed as a control section. Prior to infrared analysis, the control was examined to determine the areas of interest. Sections employed for ATR-FTIR imaging were not stained.

ATR infrared images were obtained with a PerkinElmer Spectrum Spotlight 400 infrared imaging system as previously described[13].

RESULTS

Patients

Eight patients, all males, with UA stones were studied (**Table 1**). Prior stone episodes varied from none (2 patients), 1 (1 patient), to 5 or more. In six cases, analyzed stones were virtually pure UA, the rest were mixtures of UA with CaOx. Patient 1 was exceptional in that he converted from UA to brushite stones during a period of potassium citrate treatment (**Footnote to Table 1**).

Two of the patients had undergone alkalization therapy in an attempt to dissolve their stones, but both were unsuccessful. One patient was offered dissolution therapy but declined; the other 5 patients had either acute pain or large stone burdens, such that dissolution therapy was not a good choice.

Clinical Laboratory Findings

As expected, urine pH was generally low (**Table 2**) with the exception of patient 4. The high pH in this patient is not likely due to treatment artifact as urine ammonia is not suppressed. Inadequate urine ammonia production may contribute to the pathogenesis of UA stones[14], but only patients 5 and 7 seem low compared to the urine sulfate. UA SS exceeded 1 in all but one case, compatible with the stone material. Hypercalciuria was evident in 5 patients, 4 of whom had CaOx in stones (**Table 1**).

Intraoperative Imaging and papillary grading

Renal papillae displayed a mixture of plaque and plugging (**Figure 1, Tables 3 and 4**). One papillum of patient 5 (**Figure 1, panel A**) was completely normal, consistent with his general lack of findings on papillary grading (**Table 3**) or histopathology (**Table 4**). Patient 8 (**Figure 1, panel B**) showed modest amounts of plaque (arrows) and dilated Bellini ducts (BD) (arrowhead). His papillary grading and histopathology corresponded well in showing plugs, plaque and fibrosis (**Tables 3 and 4**). Patient 4 displayed large amounts of plaque (**Figure 1, panel C, arrows**) on many papillae, as shown by a high score for plaque on both papillary grading and surface area measurement (**Table 3**). Patient 7, by contrast, illustrates very dense plaque on one papilla (**Figure 1, panel D**) but less abundant plaque on others, as noted by the discrepancy between the two measurements (**Table 3**).

In general, intraoperative papillary grading of Randall's plaque correlated with quantitative plaque surface area measurement (**Table 3)**. The Pearson correlation was 0.46, p=0.26, not significant. But the Spearman rank order correlation was 0.86, which is highly significant ($p<0.001$). Case 7 is an outlier because almost all the plaque was on one papillum, so the scoring system, by averaging, differed from the quantitation. Papillary grading of tubule deposits also corresponded with measured plug surface area, with a Spearman's correlation of 0.52 (p=0.21).

Papillary Histopathology and Mineral Analysis

Biopsies from all 8 patients showed IMCD deposits either by micro-CT (7 cases, **Table 3**) or by histopathology (7 cases**, Table 4**), consistent with intra-operative

measurements (**Table 3**). We found plaque in 5 patients (**Table 4**); of the 3 patients with no plaque on histopathology, 2 also lacked plaque by papillary surface measurements, and the third had very minimal plaque seen during intra-operative grading (**Table 3**). Interstitial fibrosis was noted in only two patients.

Figure 2, panel A illustrates apatite plugging without dilation in patient 7 (arrows). A different plug in this patient (**Figure 2, panel B**) was composed of sodium acid urate (**Table 3**). In patient 6 (**Figure 2, panel C)** tubules are dilated, with epithelial cell loss. The deposit itself was apatite. **Panel D** shows the most extensive tubule dilation and deposits we found (patient 8), accompanied by interstitial fibrosis. The crystals in the deposits were mixtures of CaOx and UA, or urate and apatite (**Table 3**). Finally, **panels E and F** illustrate two different patterns of plaque in patient 6. In **panel E** plaque is plate-like and dense in appearance, an appearance we have described previously in CaP stone formers and called novel interstitial plaque structures (NIPS)[2]. In **panel F** plaque is scattered small deposits ringing thin limbs, as typically seen.

Detailed Composition of Deposits

Micro - FTIR. Plaque deposits (**Table 4)** were apatite (not illustrated). The spectra correspond exactly to those we have obtained before.

Six patients had plugs that were studied by FTIR (**Table 3; Figure 3, panel a** illustrates patient 3**).** Five plugs contained only apatite (patients 1, 3, 4, 6, 7). Patient 7 (**Figure 3, panel b**) had another plug composed of sodium acid urate (**Table 3**). In patient 8 (**Figure 3, panel c**) we identified UA and CaOx in one plug, and apatite and urate in another (not shown).

Micro CT Analysis. Micro-CT can also identify mineral content of plugs (**Table 3**). In patient 8 we could visualize the complex topology of crystal deposits (**Figure 4**). Arrows point to deposits with x ray attenuation of purine crystals - UA or urate salts. Double arrows point to presumed apatite. Arrowheads show presumed CaOx within purine deposits. Thus various crystal forms (urate species and apatite) may coexist within plugs

Cortical Histopathology

We obtained glomeruli in 5 of the 6 cases from whom we obtained cortical tissue. Of those, global sclerosis was absent in 2 patients, found in <10% of glomeruli in 2 other patients, and found in 50% of glomeruli in the final patient. Tubule atrophy and interstitial fibrosis were absent in 4 patients, and mild in 2 others **(Table 4)**.

DISCUSSION

UA stone formers form plaque and have crystal deposits in IMCD and BD, like most stone forming phenotypes we have described[4]. Similar to other types of stone formers, tubule deposits consisted mainly of apatite, sometimes accompanied by urate salts or CaOx, despite the low pH of urine and, presumably, tubule fluid in the late nephron. Apatite is not stable at pH values below 6, which raises the question of how these tubule deposits formed. Only one patient had urine with CaP SS > 1, due to severe hypercalciuria, and he had made stones containing CaP and CaOx in addition to UA (**Tables 1 and 2**).

We previously observed this discrepancy between urine SS and tubule deposits among ileostomy patients who formed UA stones[6]. We suspect nephron heterogeneity with respect to urine pH regulation so that some terminal BD fluids have a pH above that of the bulk urine. Using intraoperative micro-electrode pH measurements in humans we have preliminary evidence that dilated BD may in fact contain high pH fluid in ileostomy patients[15]. Shock wave lithotripsy can cause significant transient high urine pH in experimental settings[16], but only two of the seven patients with apatite plugs had that modality, so the cause of tubule cell injury in the other patients is unclear.

We can compare the amount of papillary mineral in UA stone formers to that in other stone forming phenotypes that we have described (**Figure 5**). We have previously shown that Randall's plaque papillary surface area is related to urine volume, calcium and pH, and to a multivariable score describing the combined effects of these parameters[9]. UA stone formers have relatively high amounts of papillary plaque (**Figure 5, left panel**). From the micro CT analysis we can obtain quantitative measurements of number of tubule plugs per mm^2 and size of deposits in mm in papillary tissue biopsies (**Table 3, and Figure 5, right panel**). UA stone formers appear to have relatively small tubule deposit mass (**Figure 5,**

right panel); they fall into a group with cystinuria, obesity bypass, and small bowel resection patients in having scanty and small deposits. The modest mass of crystal plugging correlates well with the very mild interstitial fibrosis in the papilla and cortex of this group of patients.

The two cases (1 and 8) that display any interstitial fibrosis on papillary histopathology are also the patients with the longest duration of stone disease, and they had the largest and most numerous tubule deposits, by micro-CT. This suggests that a longer duration of stones seems related to increasing tissue mineral deposition and fibrosis.

Despite the presence of plaque and plugs we did not find any anchored stones in this series. Others have noted that UA stones are generally round and lack any kind of polar differentiation suggesting formation on an anchored site[17]. The mechanism of formation and retention of UA stones in the kidney is presently unknown.

Our results compare well with the one other study in the literature. Lieske et al studied 23 patients whose stones contained UA[18]. Of them, only 6 had stones with >80% UA so their population was mainly mixed calcium UA stones. The most pertinent comparison is between their 6 cases and our 6 cases with over 80% UA in their stones. Both groups reported plugging (5/6 and 6/6) and plaque (2/6 and 4/6, Lieske and ourselves respectively). Unlike us they found interstitial fibrosis in 3/6 cases whereas we found it only in one case who had a very long stone history (patient 8). They describe common polarizing crystals. We employed a more powerful and discriminating method and found apatite that does not exhibit birefringence. One patient did have a very large plug with CaOx in it along with UA and urate species, and this would have exhibited birefringence. Overall, we are in general agreement except for the crystal species and perhaps amount of inflammation. The fact that both this study and ours found ductal plugging in uric acid stone formers suggests that tissue damage from mineral plugging is common in this type of stone former. Such plugging might be avoided with stone preventive therapy in uric acid stone formers, but further study will be required to determine this.

This is our first opportunity to compare the assessment of papillary mineral deposits using several modalities – intra-operative papillary grading, percent surface area coverage on papillary films, micro-CT of papillary biopsies, and histopathology of papillary biopsies. The number of subjects is, of course, small, but we include these data to provide as complete a picture as possible. In general, these different assessment tools agree about the presence and abundance of plugs and plaque in patients, although they offer differing types of information. The first two methods allow an assessment of features apparent on all visualized papillae, while the latter two offer a detailed look at biopsies taken from individual papillae. It is not surprising that these different tools produce somewhat different answers about the amount and type of papillary mineral, but they appear to be complementary.

CONCLUSIONS

UA stone formers resemble those with ileostomy in forming tubule plugs that often contain crystals that form and are stable at pH values above those of their bulk urine. This suggests that there are localized tubular acidification defects permitting locally elevated pH in tubules which can support apatite crystal formation. However, the mechanism of the acidification defect is still unclear. It is notable that we saw little UA in tubule deposits, despite presumed UA SS in the distal nephron. It emphasizes our general observation that tubule mineral deposits often differ from stone composition in patients, and suggests that processes leading to tissue mineralization may differ from those that produce stones. We did not find direct evidence that UA stones form on anchored sites, leaving the mechanism of their formation an open question.

For the first time, this work permitted direct comparison between tubule plug and plaque abundance measured directly in tissue with grading estimates made during surgery. In general, grading predicted plaque and plug abundance well at the extremes - low scores went with the lowest abundances, and the obverse. Further work on more patients is needed to see how this applies to other stone phenotypes.

Overall, many findings in these patients appear to overlap with the features found in other stone phenotypes. Production of UA stones occurs when urine pH is quite low,

and CaOx stone formation may also occur if hypercalciuria is present. The reason for the low urine pH has been very well defined experimentally[14;19;20].

ACKNOWLEDGEMENTS

The work reported here was supported by NIH NIDDK P01 56788.

DISCLOSURES

The authors state that they have no conflicts of interest.

Reference List

1. Evan AP, Lingeman JE, Coe FL *et al*. Randall's plaque of patients with nephrolithiasis begins in basement membranes of thin loops of Henle. *J Clin Invest* 2003; 111: 607-616

2. Evan AP, Lingeman JE, Worcester EM *et al*. Contrasting histopathology and crystal deposits in kidneys of idiopathic stone formers who produce hydroxy apatite, brushite, or calcium oxalate stones. *Anat Rec (Hoboken)* 2014; 297: 731-748

3. Williams JC, Jr., Borofsky MS, Bledsoe SB *et al*. Papillary Ductal Plugging is a Mechanism for Early Stone Retention in Brushite Stone Disease. *J Urol* 2018; 199: 186-192

4. Coe FL, Evan AP, Lingeman JE, Worcester EM. Plaque and deposits in nine human stone diseases. *Urol Res* 2010; 38: 239-247

5. Jaeger CD, Rule AD, Mehta RA *et al*. Endoscopic and Pathologic Characterization of Papillary Architecture in Struvite Stone Formers. *Urology* 2016; 90: 39-44

6. Evan AP, Lingeman JE, Coe FL *et al*. Intra-tubular deposits, urine and stone composition are divergent in patients with ileostomy. *Kidney Int* 2009; 76: 1081-1088

7. Evan AP, Lingeman JE, Coe FL *et al*. Crystal-associated nephropathy in patients with brushite nephrolithiasis. *Kidney Int* 2005; 67: 576-591

8. Borofsky MS, Paonessa JE, Evan AP *et al*. A Proposed Grading System to Standardize the Description of Renal Papillary Appearance at the Time of Endoscopy in Patients with Nephrolithiasis. *J Endourol* 2016; 30: 122-127

9. Kuo RL, Lingeman JE, Evan AP *et al*. Urine calcium and volume predict coverage of renal papilla by Randall's plaque. *Kidney Int* 2003; 64: 2150-2154

10. Yasue T. Histochemical identification of calcium oxalate. *Acta Histochem Cytochem* 1969; 2: 83-95

11. Williams JC, Jr., Lingeman JE, Coe FL, Worcester EM, Evan AP. Micro-CT imaging of Randall's plaques. *Urolithiasis* 2015; 43 Suppl 1: 13-17

12. Zarse CA, McAteer JA, Sommer AJ *et al*. Nondestructive analysis of urinary calculi using micro computed tomography. *BMC Urol* 2004; 4: 15

13. Anderson J, Dellomo J, Sommer A, Evan A, Bledsoe S. A concerted protocol for the analysis of mineral deposits in biopsied tissue using infrared microanalysis. *Urol Res* 2005; 33: 213-219

14. Wiederkehr MR, Moe OW. Uric Acid Nephrolithiasis: A Systemic Metabolic Disorder. *Clin Rev Bone Miner Metab* 2011; 9: 207-217

15. Borofsky MS, Evan AP, Williams JC Jr. *et al*. Discovery of inappropriately alkaline micro-environments within dilated Bellini ducts: Initial evidence for heterogeneous acidification within the kidney. Journal of Endourology 29(S1), S17. 2015. Ref Type: Abstract

16. Evan AP, Coe FL, Connors BA, Handa RK, Lingeman JE, Worcester EM. Mechanism by which shock wave lithotripsy can promote formation of human calcium phosphate stones. *Am J Physiol Renal Physiol* 2015; 308: F938-F949

17. Daudon M, Williams JC Jr. Characteristics of human kidney stones. In: Coe FL, Worcester EM, Evan AP, Lingeman JE, eds. *Kidney Stones: A Multidisciplinary Approach to Diagnosis and Treatment.* Jaypee Brothers Medical Publishers, Philadelphia, PA: 2019;

18. Viers BR, Lieske JC, Vrtiska TJ *et al*. Endoscopic and histologic findings in a cohort of uric acid and calcium oxalate stone formers. *Urology* 2015; 85: 771-776

19. Bobulescu IA, Park SK, Xu LHR *et al*. Net Acid Excretion and Urinary Organic Anions in Idiopathic Uric Acid Nephrolithiasis. *Clin J Am Soc Nephrol* 2019; 14: 411-420

20. Bobulescu IA, Maalouf NM, Capolongo G *et al*. Renal ammonium excretion after an acute acid load: blunted response in uric acid stone formers but not in patients with type 2 diabetes. *Am J Physiol Renal Physiol* 2013; 305: F1498-F1503

Key for abbreviations

CaOx, calcium oxalate

CaP, calcium phosphate

CT, computed tomography

ICSF, idiopathic calcium oxalate stone formers

eGFR, estimated glomerular filtration rate

SS, supersaturation

FTIR, Fourier transform infrared spectroscopy

TABLE 1. Clinical Characteristics of Uric Acid Stone Formers

Patient	Sex	BMI	Age 1st stone	Age at biopsy	Prior stone episodes	FH	ESWL	URS	PNL	Stone analysis (%)			Past medical history				Prior treatment
										#	Uric acid	CaOx	DM	Gout	HTN	Other	
1	M	28	47	67	7	Yes	1	6	2	1*	72	28	-	-	+	-	-
2	M	33	36	37	5	No	2	0	0	1	100	0	-	-	+	-	K citrate 20 meq twice daily
3	M	45	43	43	None	No	0	0	0	1	100	0	-	-	+	Horseshoe	-
4	M	43	37	45	19	No	0	0	0	2	100	0	+	-	+	-	Sodium bicarb, K citrate
5	M	54	61	61	None	No	0	0	0	1	99	1	+	-	+	-	-

6	M	31	51	59	'very many'	No	0	0	1	2	98	2	+	-	+	-	K citrate 20 meq daily
7	M	48	55	55	1	No	0	0	0	3	57	43	+	-	+	-	-
8	M	41	34	54	8	Yes	3	3	0	1	99	1	-	+	+	-	-

FH, family history of stones; ESWL, number of extracorporeal shock wave lithotripsies; URS, number of ureteroscopies; PNL, number of percutaneous nephrolithotomies; CaOx, calcium oxalate; DM, diabetes mellitus; HTN, hypertension. *This patient's history includes a very old analysis showing uric acid stones which was followed by treatment with potassium citrate; a subsequent procedure removed stones that included the significant presence of brushite, at which point the patient was taken off of citrate therapy. This brushite history was 15 years before the study procedure described here, and there was no sign by micro CT or by infrared spectroscopy of brushite in the stone specim

TABLE 2. 24 hour urine and serum chemistries

Patient	URINE										SERUM	
	Volume L/d	pH	Calcium mg/d	Uric Acid mg/d	Citrate mg/d	Ammonia meq/d	Sulfate meq/d	SS Uric acid	SS CaOx	SS CaP	Creat mg/dL	eGFR ml/min
Normal range	> 1.5	5.8-6.2	100-200		500-750	15-50	20-80				0.8-1.2	> 90
1	1.3	5.6	447	680	920	46	49	2.31	10.61	1.73	0.77	94
2	0.8	5.7	69	468	251	17	22	2.54	5.00	0.55	1.2	77
3	1.6	5.7	221	890	221	40	62	2.29	6.50	0.63	1.07	85
4	2.5	6.2	199	681	2279	54	66	0.55	4.87	0.99	0.9	103
5	1.6	5.8	116	915	480	24	56	1.80	4.85	0.45	1.51	49
6	2.3	5.3	322	832	522	48	77	2.25	4.92	0.35	1.04	78
7	1.7	5.3	280	886	1465	33	67	3.02	8.72	0.35	0.89	96
8	1.4	5.2	214	848	407	42	41	4.00	11.93	0.39	1.04	81

TABLE 3. Papillary grading, deposit quantification and mineral type

Patient	Intra-operative Papillary Grading Scores (scale= 0-2)					Measured Surface Area		Tubular deposits by micro-CT		Mineral type in tubular deposits	
	# Papillae graded	Tubular Deposit (plugs)	Pitting	Contour	Plaque	Plug % surface	RP % surface	#/mm^2	Size (mm)	FTIR	Micro-CT
1	8	1.25	1.13	0.75	1.13	0.45	1.65	6	2.51	Apatite	Apatite, purine
2	5	1.00	0.40	0	0	0.66	0.09	2	0.23	-	-
3	5	1.20	0	0.60	0.20	0.22	0.08	1	0.20	Apatite	Apatite
4	6	0.80	0	0.70	2.00	0.17	4.08	ND	ND	Apatite	-
5	4	0.50	0	0.75	0	0.09	0.05	1	0.32	-	Apatite, purine
6	4	1.00	0.50	0	1.20	0.06	4.15	1	0.22	Apatite	Apatite, purine
7	5	0.80	0	0.20	1.20	0.24	18.6	6	0.36	1) Apatite 2) Na acid urate mono	Apatite
8	6	0.70	0.20	1.00	0.70	0.15	2.63	7	1.36	1) Ca oxalate/	1) Ca oxalate/p

										uric acid 2) Apatite/ urate	urine, 2) Apatite/p urine

SS, supersaturation; CaOx, calcium oxalate; CaP, calcium phosphate; eGFR, estimated glomerular filtration rate; RP, Randall's plaque; FTIR, Fourier transform infrared spectroscopy; micro-CT, micro computed tomography.

TABLE 4. Papillary and Cortical Histopathology

Patient	Papillary Histopathology			Cortical Histopathology			
				Glomeruli			
	Tubule Plugs	Plaque	Interstitial fibrosis	Total #	# with sclerosis	Tubular atrophy	Interstitial fibrosis
1	+	+	+	-	-	-	-
2	+	0	0	0	NA	1	1
3	+	0	0	13	1	0	0
4	+	+	0	-	-	-	-
5	0	0	0	6	0	0	0
6	+	+	0	14	0	0	0
7	+	+	0	22	2	1	1
8	+	+	+	8	4	0	0

Papillary histopathology: +, present; 0, absent. Cortical histopathology, Glomeruli: NA, not applicable; # with sclerosis, number of glomeruli present with global sclerosis. Cortical histopathology, Tubular atrophy and Interstitial fibrosis: 0, none; 1, mild or < 34% of sample.

Legends to Figures

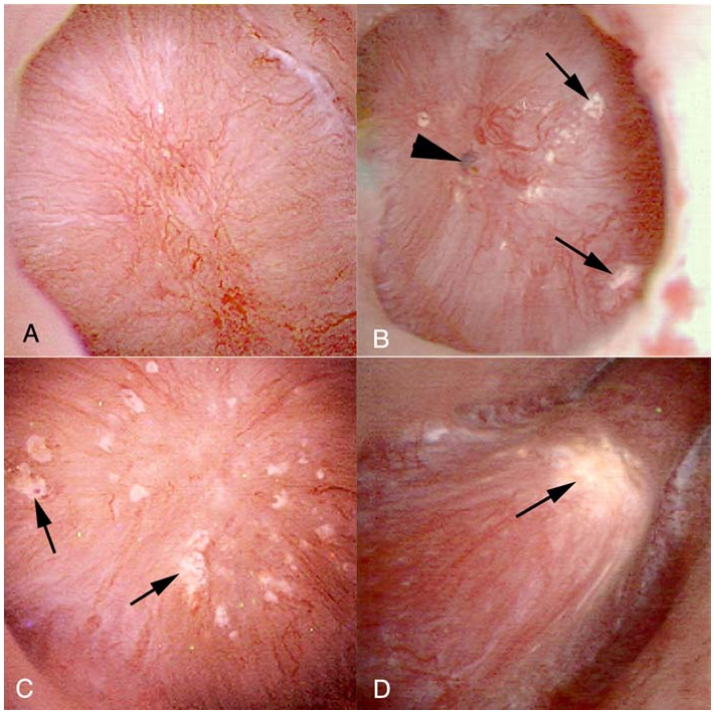

Figure 1. **Endoscopic images of papilla from uric acid stone formers**. The papillary surface of uric acid stone formers varied from normal (panel A, patient 5) to increasing area of interstitial (Randall's) plaque (panels B-D, patients 8, 4 and 7; arrows) and an occasional dilated opening of a duct of Bellini (panel B, arrowhead).

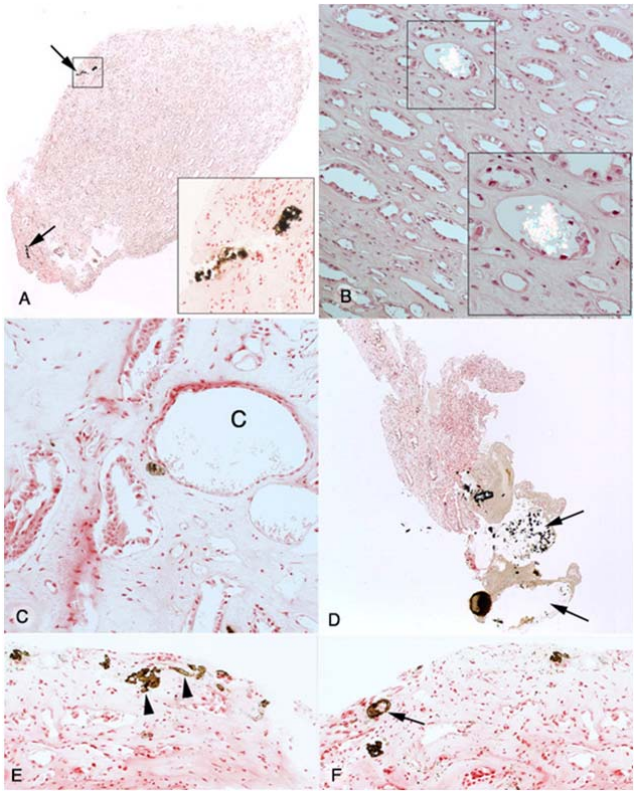

Figure 2. Histopathologic images of papillary biopsies from uric acid stone formers. The primary histologic change seen in the papillary biopsies was intraluminal plugs in IMCD without (panel A, patient 7, arrows and insert; panel B, patient 7, seen in insert) or with extensive tubular dilation (panels C and D, patients 6 and 8), labeled with a 'C' in panel C or marked with arrows in panel D). Most dilated IMCD were completely filled with mineral while a few like the IMCD labeled 'C' in panel C is partially filled. Mineral content varied from apatite (panel A, plugs seen in insert), to sodium acid urate monohydrate (panel B seen in polarizing optics, insert) to urate/apatite mix (panel D, Yasue stain) or uric acid/oxalate mix (not shown). Also seen in the interstitium were small regions of NIPS (panel E, patient 6, arrowheads) and Randall's plaque (panel F, patient 6, arrow).

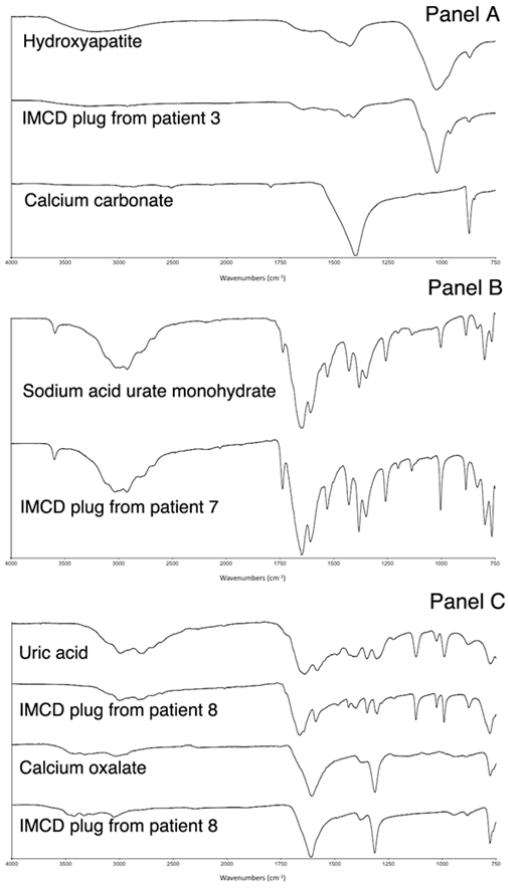

Figure 3. Micro-FTIR spectra of crystal deposits in uric acid stone formers. This figure illustrates a series of infrared spectra obtained for a set of standards (hydroxyapatite, panel a; sodium acid urate monohydrate, panel b; uric acid and calcium oxalate, panel c) and for three sites of IMCD intraluminal deposits analyzed in the papillary tissue of three different uric acid stone formers. The deposit in patient 3 has apatite, patient 7 has sodium acid urate monohydrate and patient 8 has a mixed deposit of uric acid and calcium oxalate.

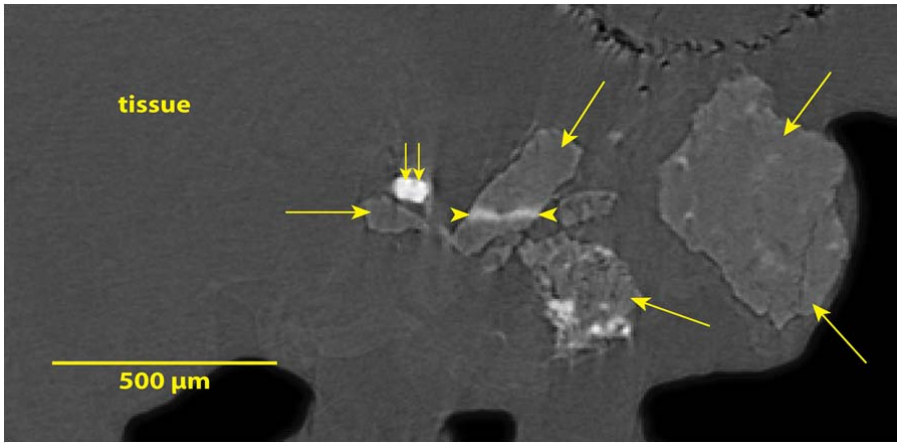

Figure 4. Micro CT image slice from papillary biopsy of uric acid stone former (patient 8). Objects brighter than tissue indicate mineral. Arrows point to mineral matching the X-ray attenuation of purine crystals (urate or uric acid). Small double arrows mark mineral with the high X-ray attenuation matching apatite. Arrowheads delineate a layer within purine mineral with X-ray attenuation consistent with calcium oxalate.

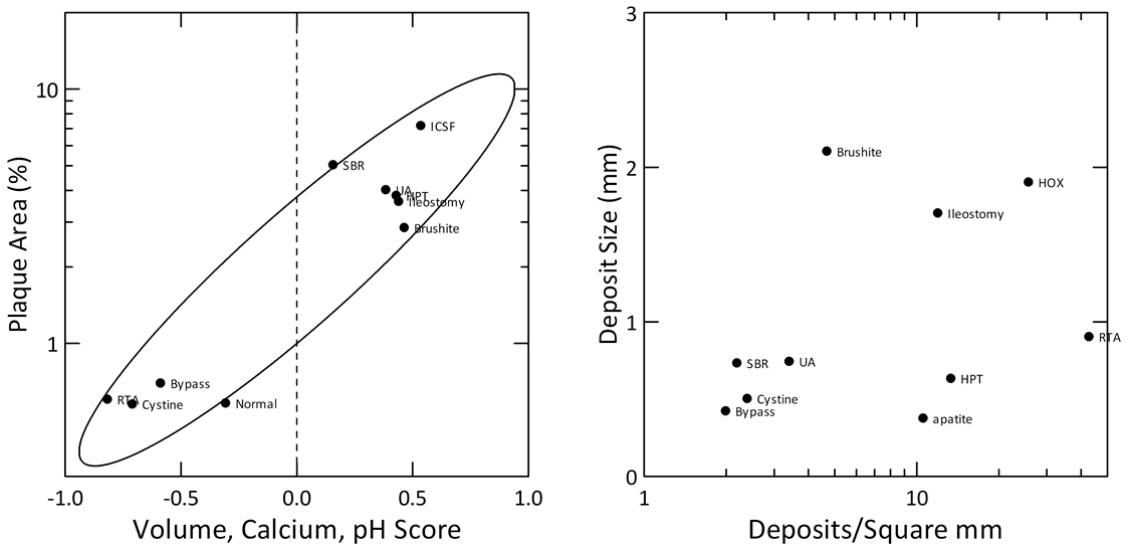

Figure 5. Comparison of papillary calcifications in UA stone formers with other stone phenotypes. Plaque surface area coverage is plotted against a multivariate score reflecting the combined effect of urine volume, calcium excretion and pH for UA, normal subjects, and eight other stone phenotypes (left panel). UA stone formers have relatively high amounts of plaque, comparable to patients with primary hyperparathyroidism (HPT) and ileostomy. Tubule deposit size and number (right panel) are plotted for the same groups. UA stone formers have modest amounts of tubule deposits and cluster with stone formers with small bowel resection (SBR), cystinuria (Cystine), and obesity bypass surgery (Bypass). Note log scale on x axis. ICSF, idiopathic calcium oxalate stone formers; RTA, renal tubular acidosis.